COMSOL CONFERENCE 2023 MUNICH

# Analysis of the stress and load distribution of an assembled screw including threaded contact

C. Hollenbeck[1] ✉ ch.hollenbeck@gmail.com
1. IMAGINE Engineering GmbH, Bergheim, Germany

## Abstract

The goal of this work is to determine reliable results of the stress and contact pressure distribution of a bolted joint using studies that are as accurate as possible in terms of material and geometry. For this purpose, a bolted joint including geometric details is considered. A 2D-axisymmetric view of the bolt opens up the possibility of very finely meshing the system and also simulating it in other respects with very high accuracy. Material nonlinearity is considered. Comparisons are made with geometrically simplified threads to show the importance of geometrical details for the accuracy of the simulation results. These and linear elastic studies for comparison show even higher notch or stress concentration effects. The most probable locations of mechanical failure of a bolted joint, namely the fillet of the first thread and the transition to the bolt head, are shown. All mechanical contact pairs are considered. A rather uneven contact pressure distribution at the washer on the bolt head is found. The load distribution on the threads simulated in this work is more uniform than others have determined. Additional studies with other shapes of nuts and modified threads are conducted to identify ways to equalize the thread pressure distribution.

**Keywords:** FEM, FEA, nonlinearity, plasticity, mechanical contact, Lagrange multiplier, notch effect, stress concentration, thread contact

## Introduction

There are different possibilities to simulate a bolted joint. If only the connection of parts in an assembly with the stress distribution and surface pressure between the components without the bolt itself is of interest, the thread of the bolt is omitted and only the effect of bolted connections on an assembly is calculated.
Here in this work, the thread of the screw is included because the thread contact pressure besides the stress distribution is of great interest to analyze the screw itself. In accordance with VDI Guideline 2230 Sheet 2, simulations are performed here according to model class IV as the most accurate and demanding model class. Several studies are compared with each other. Geometrically and materially simplified studies are compared with more accurate studies including physical nonlinearity and anyway geometrical nonlinearity due to geometrical contact. Very detailed insights into the stress and contact pressure characteristics of all areas of the bolted joint are given.

## Geometry

At the beginning, a screw of the type M12 with a simplified, automatically generated 3D thread was designed with SOLIDWORKS® (see Fig. 1 (left)). This thread does not contain root radii resp. core fillets. The pitch angle of the 3D-thread with respect to the horizontal is only about $\varphi \approx \arctan(P/(\varnothing_{\text{flank}} \cdot \pi)) = \arctan((1.75\ \text{mm})/(10.8633\ \text{mm} \cdot \pi)) \approx 2.94\ °$.
This angle is close to zero and it seemed reasonable to make a 2D-axisymmetric simplification.

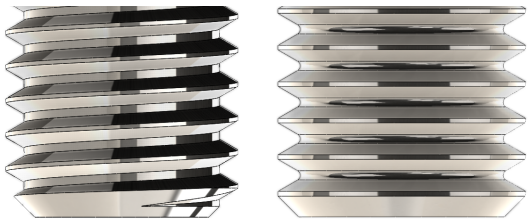

*Figure 1. 3D – thread with simplified contour (left) and 2D – thread with root radii or core fillets (right)*

This 2D-axisymmetric simplification (see Fig. 1 (right)) opened up the possibility of meshing the geometry very finely and also to consider several variants including nonlinearity of the material, too.
Theoretically, an M12-screw might have a diameter of exactly 12 mm, but it is normally smaller due to common tolerances. Here a diameter of the screw with 11.9 mm has been chosen. This diameter is within the tolerance field '6h' with a minimum to maximum dimension of 11.735 mm to 12 mm. This diameter is also within the tolerance field '6g' with a minimum to maximum dimension of 11.701 mm to 11.966 mm. The corresponding root radii are $r_{\text{screw}} = 0.253$ mm und $r_{\text{nut}} = 0.126$ mm. These radii are not just small geometric details, they have a very strong effect on the level of the notch effect or stress concentration. For the pitch of the thread the default value of $P = 1.75$ mm has been chosen. An assembly of a 2D-axisymmetric bolt similar to a Hexagon socket screw has been constructed, which is per se more similar to a 2D axisymmetric shape than a hexagon head bolt. The M12 × 60 mm screw is mounted in a through hole with a diameter of $\varnothing_{\text{hole}} = 13$ mm.

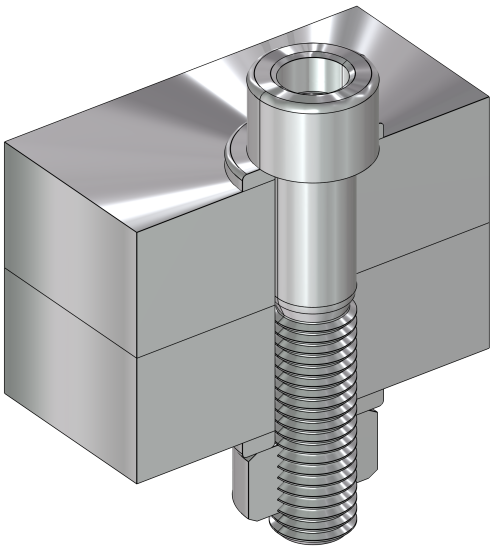

*Figure 2. 3D – CAD – assembly as a basis for the simulation (system in halved view to be able to see the screw)*

This assembly contains besides the screw one nut, two washers and two blocks of metal (see Fig. 2). In the simulation, a vertical sectional view of this assembly was used as geometric basis for the simulation.

## Material Properties

Linear elastic simulations follow the simple equation $\sigma = \varepsilon \cdot E$. The mechanical stress $\sigma$ increases linearly as function of the strain $\varepsilon$, if the Young's modulus $E$ is constant and this is the case for linear elastic studies. Here in this work, it is simulated materially nonlinearly and some studies are additionally calculated in linear elastic for comparison.
A bolt with steel as material and a strength class of 10.9 has been considered. That means, that the ultimate tensile strength (UTS) has a value of $R_m = 1000$ N/mm$^2$. The 0.2 % yield strength is 90 % of this value, i. e. $R_{p0.2} = 900$ N/mm$^2$. The Young's modulus is $E = 2 \cdot 10^5$ N/mm$^2$ = 200 GPa. The Poisson's ratio is $\nu = 0.3$. A strain of $\varepsilon = 0.65$ % = (0.45 + 0.2) % = $R_{p0.2} / E$ + 0.2 % occurs, if the 0.2% yield strength is reached and 0.2 % of this strain is inelastic or plastic, so this part of the strain does not disappear after mechanical unloading. For high-tensile steels, the uniform elongation is in the range of 5 % to 6 %. Here for this study, a uniform elongation of $A_g = 5.45$ % is chosen.

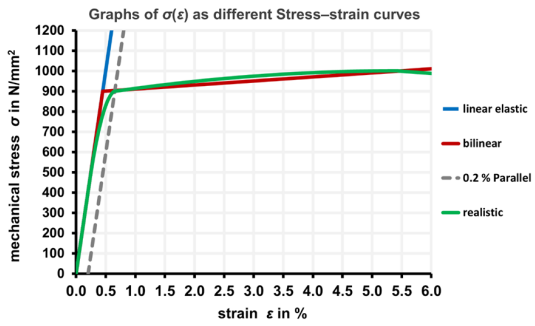


*Figure 3. Graph with different stress-strain-curves*

Especially for metals with a 0.2% yield strength which is close to the UTS, a bilinear model of the stress-strain curve seems to be an approach with small deviations to the reality (see Fig. 3). In this way, an isotropic hardening is implemented. With the assumed values, a so-called isotropic tangent modulus of $E_T = 2$ GPa $= 0.01 \cdot E$ is calculated. This is the slope of the bilinear model of the stress-strain curve in the plastic range. This slope is by 99 % lower than the Young's modulus. That means, that the stress only slowly increases in the nonelastic or plastic range. For example, a strain of $\varepsilon = 1$ % is present when a stress of 911 N/mm$^2$ is reached in the bilinear model. For the same strain, the linear model leads to a stress of 2000 N/mm$^2$ which is much too high compared to reality.
The stress cross-sectional area is reduced because of the thread and a preload force of
$F_{pretension} = R_{p0.2} \cdot 0.25 \cdot \pi \cdot (d_{core})^2 =$
900 N/mm$^2$ $\cdot$ 0.25 $\cdot$ $\pi$ $\cdot$ (9.853 mm)$^2$ $\approx$ 68.6 kN
is calculated, if an average stress of 900 N/mm$^2$ corresponding to the 0.2 % yield strength should occur in the core cross-section of the screw. The screw should therefore be loaded with significantly less than a pretension force of $F_{pretension} = 68.6$ kN. Here in these simulation studies, loads of up to 75 kN and above were also applied in order to be able to see nonlinear effects in the range of this very high load.

## Numerical Model

All mechanical contact pairs were considered numerically. That are eleven contact pairs in total with six contact pairs at the single thread flanks. All of the simulations presented here in this work are geometrically nonlinear because of considering these contact pairs. In COMSOL®, each contact pair has a so-called source and destination. Beside other aspects, the mechanically stiffer side should be assigned to the source and the destination should be meshed finer compared to the source by at least a factor of two [1]. Here the destination boundary resp. line was meshed finer by a factor of three. The side length of the tetrahedral finite elements at the threads has been set to a value of $\Delta s = 10$ µm (see Fig. 4). The contact length at each thread has a value of $\Delta l \approx 1036$ µm, thus a number of about 104 elements can be placed there. This is an extremely fine mesh with a number of elements for the whole geometry of $n = 0.138277$ Mio. in total. Additionally, a value of $\Delta s = 30$ µm has been chosen for a comparison to a coarser, but in general also fine mesh ($n = 0.037459$ Mio. FE-elements in total).
In [2, p. 138] it is stated, that linear [discretized] tetrahedral elements are the worst which can be chosen, because each is mechanically very stiff itself. The default setting of the discretization in structural mechanical simulations in COMSOL® is 'quadratic serendipity'. Here an even higher discretization of 'Lagrange 3rd order' (or 'Cubic Lagrange' in older versions) has been chosen, which is far beyond 'linear'.

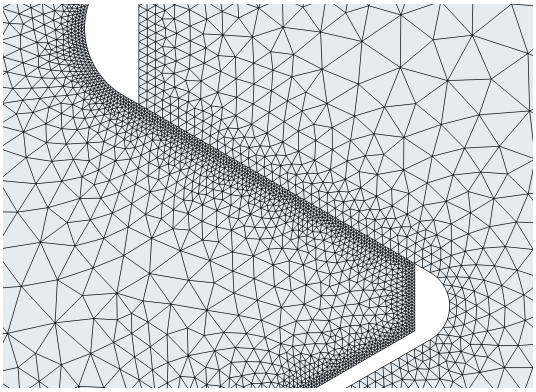

*Figure 4. Part of the FE-Mesh at one thread flank*

For comparison a FE-mesh with exclusively quadrilateral elements has been set up additionally with the same increased discretization (with $\Delta s$ = 20 µm at the threads and $n$ = 0.087206 Mio. FE-elements in total). These quadrilateral or hexahedral (in 3D) meshes are more commonly used in other FE software's. In addition, the optional settings "Calculate boundary flows" and "Apply smoothing to boundary flows" have been activated in all simulations. All contact pairs were defined with the contact method "Augmented Lagrangian" in contrast to the less accurate "Penalty" method. In [3, p. 263] it is stated, that the Lagrange multiplier is the same as the contact force and in [2, p. 229] it is mentioned, that displacements correspond exactly to the analytical solution using the method of Lagrange Multiplier in the context of mechanical contact in FEM-studies. The initial value of the contact pressure is set to $T_n$ = 0 N/m$^2$ for all mechanical contact pairs, which is the default value. This makes sense in combination of ramping up the pretension in an auxiliary sweep beginning with a pretension of $F_{pretension}$ = 0 kN and increasing it in small steps to reach convergence. Then there are appropriate initial values available for each intermediate step in this so-called 'Continuation method'. The preload is induced in an intermediate plane resp. horizontal line of the screw about 5 mm above the last thread (see Fig. 5) using the subnode 'bolt pretension' as a global setting.

In general, the physics "structural mechanics" has been used obviously. By default, it is calculated linear elastically. In the model builder of COMSOL® the subnode "plasticity" of the node "linear elastic material" was chosen to implement the isotropic tangent modulus of $E_T$ described before in the section "Material Properties" to realize the physical nonlinearity and to deactivate the linear calculation.

Friction makes the simulation even more nonlinear. Source [2, p. 234] describes that the Lagrange multiplier method in combination with friction should only be used when very high accuracies are required due to increased computational effort and lower convergence probability. This work has the requirement of very high accuracy, so in one study the Lagrangian method was combined with friction (friction coefficient of $\mu$ = 0.1) for comparison. The other studies, on the other hand, have been simulated without friction losses.

The simulation with the coarser tetrahedral mesh converged up to a preload of $F_{preload}$ = 85 kN with a calculation time of $\Delta t_{calc}$ = 11 h 42 min and a physical memory requirement of 5.09 GB RAM. The simulation with quadrilateral mesh converged up to a preload of $F_{preload}$ = 81 kN with a calculation time of $\Delta t_{calc}$ = 18 h 2 min and a memory requirement of 17.64 GB RAM (> 16 GB RAM). The simulation with the finer tetrahedral mesh converged up to a preload of $F_{preload}$ = 77 kN with a calc. time of $\Delta t_{calc}$ ≈ 20 h (manually stopped because of slow convergence) and a memory requirement of 13.15 GB RAM. The calculations were performed with an Intel® Core™ i7-10750H processor.

## Simulation Results

Several areas of the simulated geometry are of interest for a detailed presentation. An overview of the entire geometry of the nonlinear study for a high preload force with representation of the equivalent stress according to von Mises is displayed in Fig. 5. Large stresses can be seen in the area of the thread and in the area of the transition of the bolt to the screw head. Certain areas, such as the thread contact between the screw and the nut, are particularly interesting and will be shown in more detail in the following.

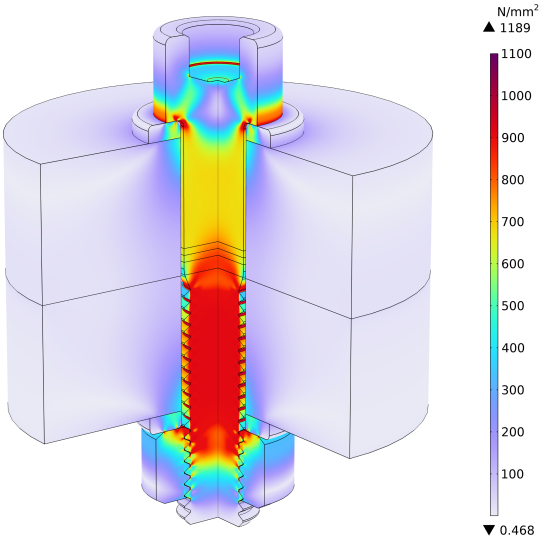


*Figure 5. Nonlinear calculation; $F_{preload}$ = 75 kN; simulation result spanned by $\varphi$ = 270° with display of the equivalent stress according to von Mises (color scale limited to $\sigma_v \leq$ 1100 N/mm$^2$ for direct comparability to other simulation results) [fine tetrahedral mesh]*

In Fig. 6, the equivalent stress is displayed for a preload of $F_{preload}$ = 50 kN. In the area of the first thread, the highest stresses occur in the rounded transitions to the other threads. The max. stress occurs in the upper fillet of the first thread and has a value of $\sigma_v \approx$ 929 N/mm$^2$ > $R_{p0.2}$, so this mechanical load is locally already in the plastic range.

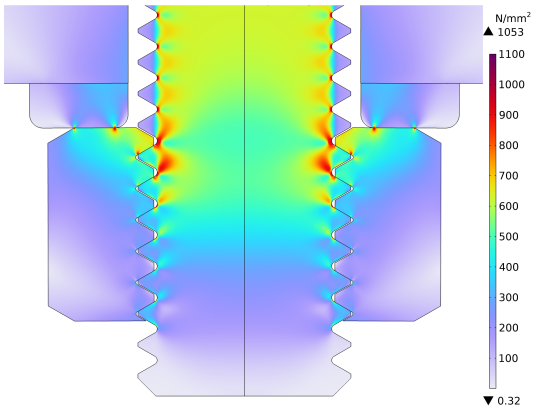


*Figure 6. Nonlinear calculation; $F_{preload}$ = 50 kN; equivalent stress according to von Mises [fine tetrahedral mesh]*

A linear elastic calculation leads to a value of $\sigma_v \approx$ 2330 N/mm² ≈ 2.51 · 929 N/mm² at the same location. In Fig. 7, the equivalent stress is displayed for a very high preload of $F_{preload}$ = 75 kN. Here it is also the case, that the highest stress related to the screw with a value of $\sigma_v$ = 1018.21 N/mm² occurs in the fillet of the first thread flank. In comparison to this, the coarser tetrahedral mesh outputs a value of 1018.50 N/mm². The sharp geometry transitions at the nut in contact to the washer lead to extreme stresses very locally concentrated as this is marked in Fig. 7, but these stress concentrations do not occur at this level for the coarser mesh.

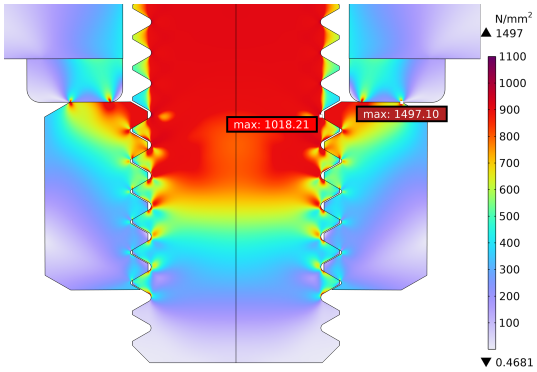


*Figure 7. Nonlinear calculation; $F_{preload}$ = 75 kN; equivalent stress according to von Mises [fine tetrahedral mesh]*

In Fig. 8, the equivalent stress is displayed for the same very high preload of $F_{preload}$ = 75 kN having simulated linear elastically. Here stress concentrations due to the notch effect are very clearly visible at the roots of the thread flanks. In the case of the linear elastic model, the stresses can increase to very high values, while in the nonlinear model they cannot increase by far to such an extent due to the onset of plasticization. The max. stress in the fillet of the first thread has a value of $\sigma_v \approx$ 3512 N/mm² ≈ 3.45 · 1018 N/mm² (see marking in Fig. 8).

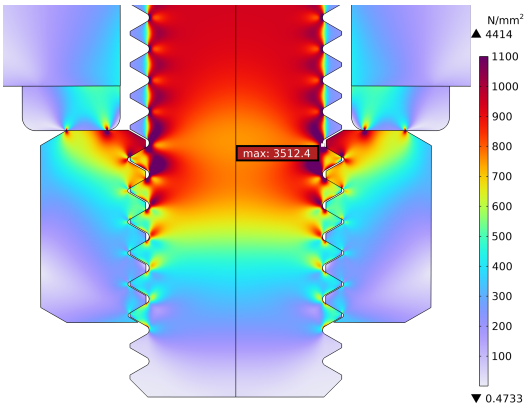


*Figure 8. Linear elastic calculation; $F_{preload}$ = 75 kN; equivalent stress according to von Mises [fine tetrahedral mesh]*

In Fig. 9, a linear elastic simulation result for a geometry without root radii resp. fillets or roundings at the thread bases is to see. Here a maximal stress of 14423 N/mm² ≈ 4.11 · 3512 N/mm² ≈ 14.17 · 1018 N/mm² occurs, which is far beyond the ultimate tensile strength. This results here because of an increased notch effect due to sharp-edged, geometric transitions. The max. von Mises stress for $F_{preload}$ = 50 kN is $\sigma_{max}$ = 9359.7 N/mm² ≈ 0.649 · 14423 N/mm² ≈ 50 / 75 · 14423 N/mm².

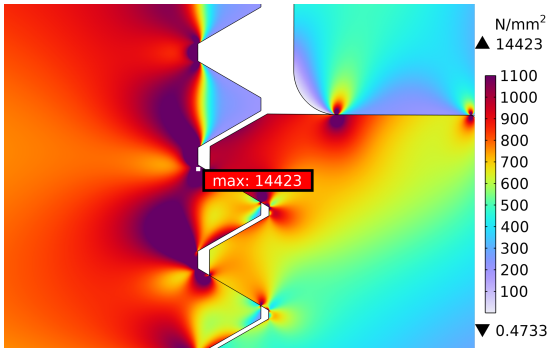


*Figure 9. Linear calculation; $F_{preload}$ = 75 kN; equivalent stress according to von Mises; without root radii [fine tetrahedral mesh]*

This shows that omitting supposedly unimportant geometrical details can lead to much higher local peak stress values due to extremely increased notch effects.
In the following, the three different FE-meshes are compared for the same preload force of $F_{preload}$ = 70 kN on a partial section of the geometry. For all three cases, a max. equivalent stress of $\sigma_v \approx$ 971 N/mm² can be seen in the fillet of the first thread (for more precise values: see markings in the Figures 10 – 12). The still fine tetrahedral mesh, which is significantly coarser only in direct comparison, thus seems to be just as suitable for precise results.

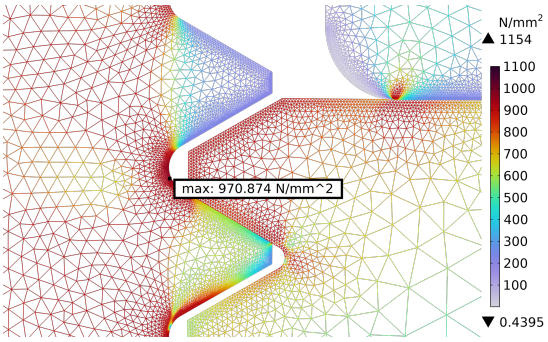


*Figure 10. Nonlinear calculation; $F_{preload}$ = 70 kN; equivalent stress according to von Mises; [fine tetrahedral mesh]*

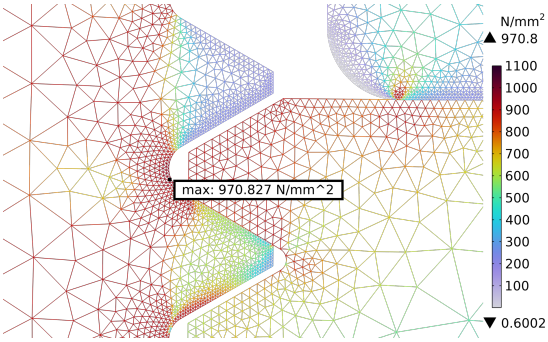


*Figure 11. Nonlinear calculation; $F_{preload}$ = 70 kN; equivalent stress according to von Mises; [coarser tetrahedral mesh]*

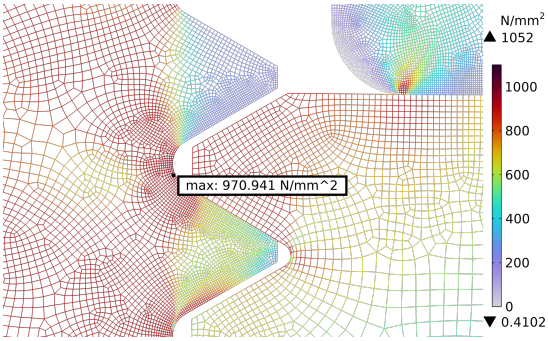


*Figure 12. Nonlinear calculation; $F_{preload}$ = 70 kN; equivalent stress according to von Mises; [quadrilateral mesh]*

However, the equivalent stress peak values differ at the contact of the nut to the washer in very small local areas. This is why there are different max. values to see at each end of color scale in Fig. 10 – 12.
Another interesting part of the simulated geometry is the head of the bolt and the area in its ambience also with contact pairs. In the fillet of the transition from the bolt to the screw head, a strong notch effect also occurs here (radius modeled with $r$ = 1 mm). In addition to the equivalent stress, Fig. 13 also shows the contact pressure of two pairs of contacts. At the edges of the screw head contact surface, there is a strong contact pressure increase radially inwards and outwards (see Fig. 13 & 14). The high surface pressures would damage, notch or scratch the contact surface. The washer with a contact surface that is larger by a factor of ≈ 3.58 significantly reduces the contact pressure and thus fulfills its purpose of not damaging the component. However, the peak contact pressure of 469 N/mm² occurring radially on the inside of the washer is 3.00 times larger than the average contact pressure of
$T\varnothing = (50\ \text{kN}) / (\pi \cdot (12^2 - 6.5^2)\ \text{mm}^2)$
$= 156.42\ \text{N/mm}^2$. The simulation has been performed without friction ($\mu = 0$). Surprisingly, the radially outer region of the washer lifts off the bearing or contact surface, resulting in zero contact pressure over a fairly large area (see Fig. 15). Analytical calculations would only provide the average values without detecting the extreme distribution. The maximal gap distance between the outer diameter of the washer to the metal block is $\Delta z_{gap}$ = 2.134 µm for a preload of $F_{preload}$ = 50 kN.

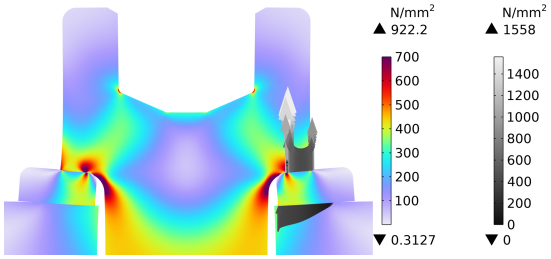


*Figure 13. nonlinear calculation; $F_{preload}$ = 50 kN; equivalent stress according to von Mises (left scale) & contact pressure (right scale); displacement exaggerated by 25 times [coarser tetrahedral mesh]*

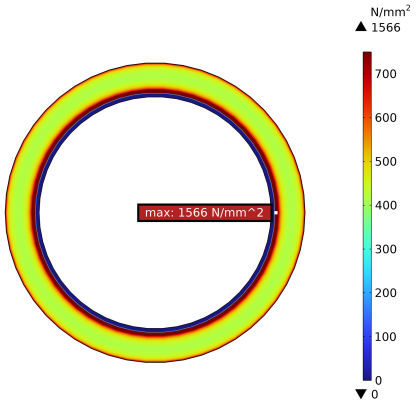


*Figure 14. nonlinear calculation; $F_{preload}$ = 50 kN; contact pressure at the screw head contact surface to the washer [coarser tetrahedral mesh]*

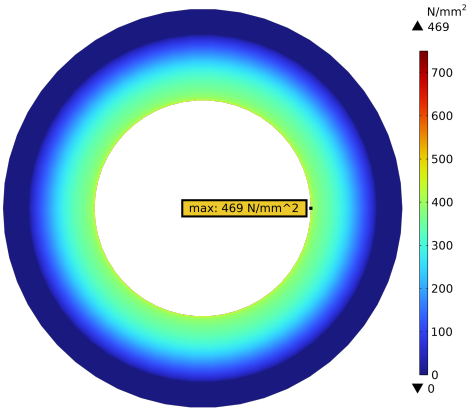


*Figure 15. nonlinear calculation; $F_{preload}$ = 50 kN; contact pressure at contact surface of the washer to the metal block [coarser tetrahedral mesh]*

The simulation results of the contact pressure distribution on the threads for different variants are presented below.
It can be seen qualitatively that the contact pressure on the first threads is higher than on the deeper threads (see Fig. 16). The load distribution between the individual threads can be seen quantitatively in Table 1. Surprisingly, the average contact pressure or load on the last ($6^{th}$) thread is greater than that of the penultimate ($5^{th}$) thread.
If very large preload forces are applied, the load distribution between the threads becomes significantly more uniform. When an extremely large preload force of $F_{preload}$ = 85 kN is applied, plastic effects dominate. The screw would fail mechanically before reaching this preload force, but this result (see Fig. 17 r.) could be determined by simulation. In this figure it can be seen that the displacement is so large that the distance between the first two threads of the bolt and the internal thread of the nut significantly increases. The displacement has been set realistically with a deformation scaling factor of '1'. For this preload of 85 kN the load distribution does not lead to perfectly balanced load shares of $\varphi_i = 1/6 \approx 16.67$ %. (see Tab. 1).

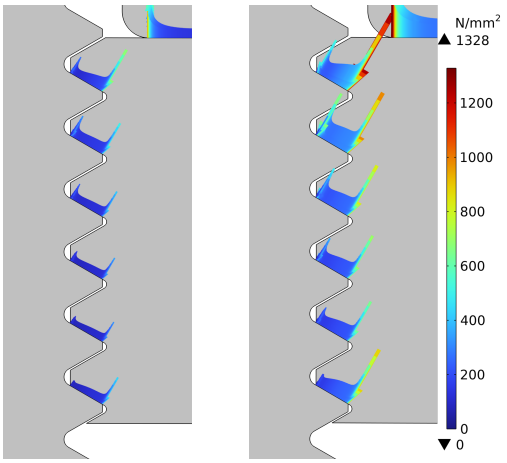


*Figure 16. contact pressure at threads: nonlinear calculation with a preload of* 25 kN *(left) &* 50 kN *(right)*

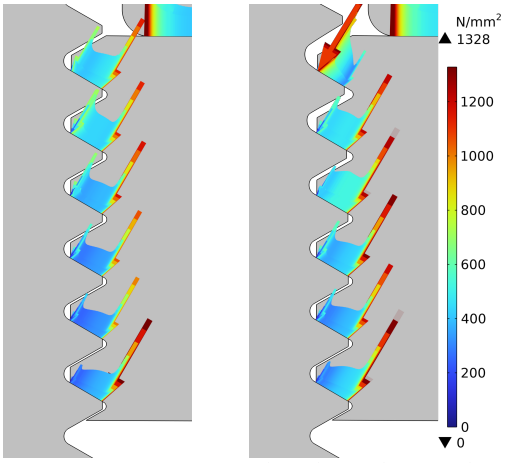


*Figure 17. contact pressure at threads: nonlinear calculation with a preload of* 75 kN *(left) &* 85 kN *(right)*

According to the simulation, the load share of the first thread is $\varphi_1 = 21.4$ % [for $F_{preload} = 25$ kN (linear effects dominate)]. This is significantly less than the value of approximately 28 % determined by Yang et. al. [4]. A cause for this rather large difference was sought. An additional simulation was carried out with omission of the washer at the nut. This study showed a larger load share of the first thread of $\varphi_1 =$ 23.9 % (see Tab. 2 & Fig. 18 l.). This can be explained by the fact that the force flow without washer has to cover a shorter distance to the first thread, i. e. the force is applied more directly, but this is still less than 28 %. One reason for this deviation could be that the through hole in [4] is modeled with $\varnothing_{hole*} \approx 12$ mm $< \varnothing_{hole} = 13$ mm and this dimensioning is not standard, so the force can flow even more directly with more radially inner contact surface.

| | Load shares of the individual threads (The 1st thread is the top one in Fig. 16 & 17) | | | | | |
|---|---|---|---|---|---|---|
| $F_{pretension}$ in kN | 1st | 2nd | 3rd | 4th | 5th | 6th |
| 25 | 21.4 % | 20.5 % | 16.5 % | 13.9 % | 12.8 % | 14.9 % |
| 50 | 21.1 % | 20.5 % | 16.6 % | 14.0 % | 12.9 % | 15.0 % |
| 75 | 19.4 % | 19.9 % | 17.1 % | 14.6 % | 13.5 % | 15.5 % |
| 85 | 18.1 % | 16.9 % | 18.9 % | 15.9 % | 14.2 % | 16.0 % |

*Table 1. Load distribution for different pretensions (coarser tetrahedral mesh)*

A study including friction at all contact pairs with a coefficient of friction of $\mu = 0.1$ with a slightly higher load share of the first thread has been added (see Tab. 2).

| | Load shares of the individual threads | | | | | |
|---|---|---|---|---|---|---|
| note | 1st | 2nd | 3rd | 4th | 5th | 6th |
| incl. washer | 21.1 % | 20.5 % | 16.6 % | 14.0 % | 12.9 % | 15.0 % |
| without washer | 23.9 % | 20.6 % | 16.0 % | 13.2 % | 12.1 % | 14.1 % |
| incl. $\mu = 0.1$ | 22.0 % | 21.0 % | 16.5 % | 13.5 % | 11.9 % | 15.0 % |
| nut in Alu | 17.7 % | 19.7 % | 16.3 % | 14.2 % | 13.9 % | 18.2 % |
| nut in Ti | 18.7 % | 19.9 % | 16.4 % | 14.2 % | 13.7 % | 17.1 % |

*Table 2. Load distribution of different variants for* 50 kN *(friction with* $\mu$ = 0.1 *incl. washer; nut in Alu & Titanium calculated in linear elastic incl. washer)*

It is to be expected that a mechanically less stiff nut will lead to a more uniform contact pressure distribution. This has been simulated in an additional study in the form of a nut made of aluminum with a Young's modulus of $E_{Alu} = 70$ GPa $= 0.35 \cdot E_{steel}$. The densities have almost the same relative relationship of $\varrho_{Alu} = 2700$ kg/m$^3 \approx 0.34 \cdot \varrho_{steel}$. In the simulation, source and destination were swapped in the contact pairs and, accordingly, the FE meshing. The load distribution is clearly more uniform when comparing the threads with each other (see Tab. 2), but the contact pressure distribution per individual thread deviates far from a constant profile with an approximately triangular profile. Surprisingly, especially the first and last thread are not fully engaged (see

Fig. 18 r.). In [4] one calculation is performed for $E^* = 1/3 \cdot E_{steel}$. This Young's modulus $E^*$ is very close to $E_{Alu}$ (s. above). In [4] a load share of the first thread for this reduced Young's modulus of $\varphi_{1^*}$ = 29.2 % is calculated (for '2D FEA'), but the density is probably not reduced in this work. Anyway, there is a large difference between this load share and the load share calculated here in this paper of $\varphi_1$ = 17.7 %.
A nut made of titanium (Ti) with a Young's modulus of $E_{Ti}$ = 105 GPa and a density of $\varrho_{Ti}$ = 4500 kg/m³ has been added (see Tab. 2, last row).

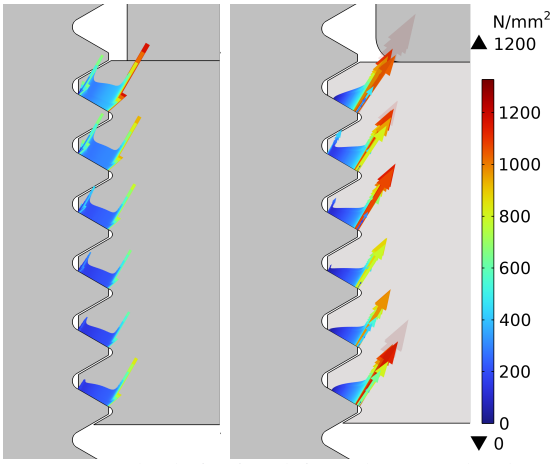


*Figure 18. preload of* 50 kN*; left: nonlinear steel without washer; right: linear elastic calculation with nut in Aluminum (color scale directly comparable to Fig. 16)*

## Additional Studies

The simulation studies up to this point appeared to be so interesting especially concerning the subject of contact pressure distribution at the threads that this paper is expanded to include other nuts with more uniform contact pressure distribution in the following. In Fig. 19, a tension nut (in German: 'Zugmutter') is shown [5, p. 228]. A suggested load distribution, which might be analytically calculated or estimated is to see in the same figure. There are similar geometries and load distributions to see in the sources [6, p. 205] and [7, p. 315].

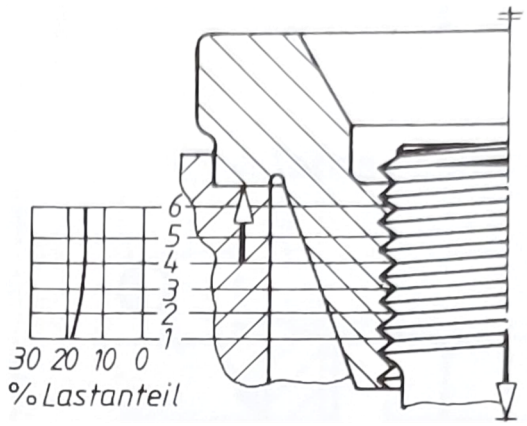


*Figure 19. tension nut ('Zugmutter') with load distribution or load share ('Lastanteil')*
*[source for this illustration: [5, p. 228]]*

This type of nut has been modeled in CAD with the same type of thread (M12) with the same tolerance as before and steel as material.
The simulated resulting pressure distribution of the threads is illustrated in Fig. 20.

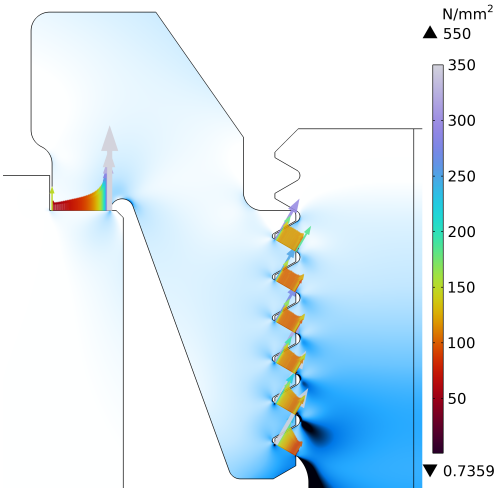


*Figure 20. tension nut; linear calc. for* 25 kN*; Display of the contact pressure distribution incl. illustration of the equivalent stress in the background*

According to the simulation, a contact pressure distribution resp. a load distribution can be seen in Table 3 for the simulated tension nut.

| Load shares of the individual threads for a tension nut corresponding to Fig. 20 | | | | | |
|---|---|---|---|---|---|
| 1st | 2nd | 3rd | 4th | 5th | 6th |
| 17.2 % | 17.9 % | 16.9 % | 15.7 % | 15.3 % | 17.0 % |

*Table 3. Load shares of the simulated tension nut (linear elastic simulation for a preload of* 25 kN *for steel)*

This simulated load distribution is comparable to the thread pressure distribution outlined in Fig. 19.

Another screw nut with an expected more even load distribution compared to a default nut is a ring-shaped screwed-in nut resp. an annularly screwed-in nut to redirect the flow of force (see Fig. 21).

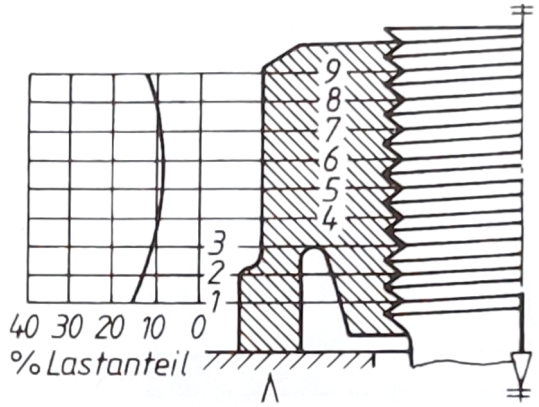


*Figure 21. ring-shaped screwed-in nut resp. annularly screwed-in nut [source for this illustration: [5, p. 228]]*

The simulated resulting pressure distribution of the threads is displayed in Fig. 22.

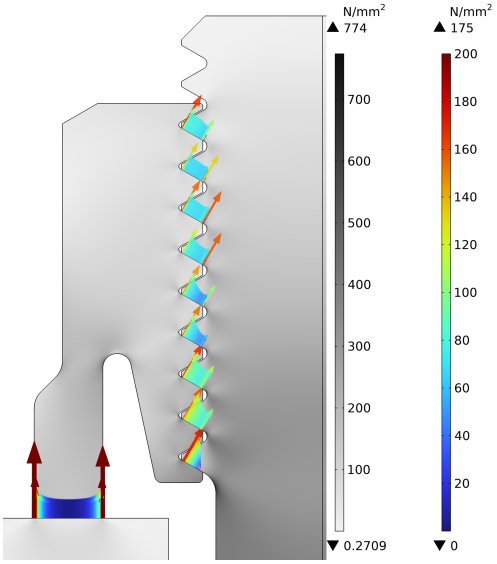


*Figure 22. annularly screwed-in nut; nonlinear calc. for* 25 kN; *display of the contact pressure distribution (scale r.) incl. illustration of the equivalent stress in the background (scale l.) [geometry more similar to [7, p. 314]]*

The simulated load distribution can be seen in Table 4 for the simulated annularly screwed-in nut.

| Load shares of the individual threads for an annularly screwed-in nut corresponding to Fig. 22 | | | | | |
|---|---|---|---|---|---|
| 1st | 2nd | 3rd | 4th | 5th | 6th |
| 11.1 % | 15.1 % | 13.6 % | 9.96 % | 9.75 % | 10.7 % |
| 7th | 8th | 9th | | | |
| 10.2 % | 9.42 % | 10.3 % | | | |

*Table 4. Load shares of the simulated annularly screwed-in nut (nonlinear for a preload of* 25 kN *for steel)*

This simulated load distribution is broadly comparable to the thread pressure distribution to see in Fig. 21.

Another screw connection with an expected more even load distribution is the so-called Solt-thread [5, p. 228]; [8].

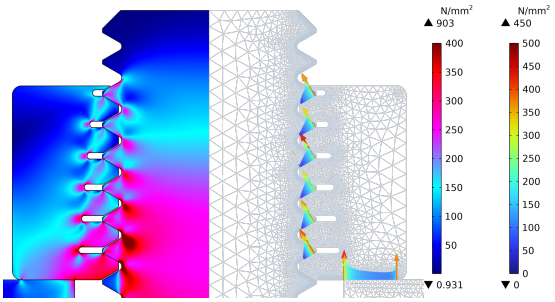


*Figure 23. nut with Solt-thread: equivalent stress (von Mises) displayed (l.) and contact pressure & mesh (r.)*

| Load shares of the individual threads for a nut with Solt-thread corresponding to Fig. 23 | | | | | |
|---|---|---|---|---|---|
| 1st | 2nd | 3rd | 4th | 5th | 6th |
| 17.6 % | 17.9 % | 16.8 % | 15.8 % | 15.2 % | 16.6 % |

*Table 5. Load shares of the Solt-thread (nonlinear for a preload of* 25 kN *for steel) corresponding to Fig. 23*

This specific design of a Solt screw connection shows an almost uniform contact pressure distribution (see Tab. 5). The long threaded bars have a springy effect. The threads are therefore geometrically softer and the contact pressure profile is similar to the simulation result with aluminum as the material of the nut (compare Fig. 23 to Fig. 18).

## Conclusions

Very detailed insights into the stress distribution in the components of a screw were obtained. As expected, it was shown that a bolted joint is most likely to fail mechanically at the first thread or at the fillet at the bolt head. Studies comparing linear elastic considerations and geometric simplifications with omission of core fillets have shown even much stronger notch resp. stress concentration effects compared to more realistic nonlinear simulations. Detailed insights into the contact pressure distribution have surprisingly shown that a washer is not completely in contact with the bearing surface under load. The contact pressure distribution at the metric threads simulated here in this work has shown a more uniform load distribution than values determined in other papers or textbooks. Several variants of simulations have given detailed insights into the shape of the contact pressure at the threads.

## References

[1] COMSOL®, "Structural Contact Modeling Guidelines", COMSOL Multiphysics®, [Online]. Available: https://www.comsol.de/support/knowledgebase/1102. [Accessed 7th April 2023].

[2] L. Nasdala, FEM-Formelsammlung Statik und Dynamik, 3rd ed., Springer Vieweg, 2015.

[3] W. Rust, Nichtlineare Finite-Elemente-Berechnungen, 3rd ed., Springer Vieweg, 2016.

[4] G. Yang et. al., "Three-dimensional Finite Element Analysis of the Mechanical Properties of Helical Thread Connection", 2013.

[5] H. Wittel, D. Muhs, D. Jannasch and J. Voßiek, Roloff/Matek Maschinenelemente, 19th ed., Vieweg+Teubner, 2009.

[6] G. Niemann, Maschinenelemente Band I, 2nd ed., Springer-Verlag, 1981.

[7] H. Hinzen, Maschinenelemente 1, 1st ed., Oldenbourg, 2000.

[8] E. Jaquet, "Ueber eine neuartige Schraubenverbindung.", Zeitschrift: Schweizerische Bauzeitung, 1931.